Atmos. Chem. Phys. Discuss., 4, 4191–4225, 2004
www.atmos-chem-phys.org/acpd/4/4191/
SRef-ID: 1680-7375/acpd/2004-4-4191

Atmospheric Chemistry and Physics Discussions

Actinic flux and O^1D photolysis frequencies retrieved from spectral measurements of irradiance at Thessaloniki, Greece

S. Kazadzis[1], C. Topaloglou[1], A. F. Bais[1], M. Blumthaler[2], D. Balis[1], A. Kazantzidis[1], and B. Schallhart[2]

[1]Laboratory of Atmospheric Physics, Aristotle University of Thessaloniki, Greece
[2]Institute for Medical Physics, University of Innsbruck, Austria

Received: 25 May 2004 – Accepted: 30 June 2004 – Published: 4 August 2004

Correspondence to: S. Kazadzis (skaza@skiathos.physics.auth.gr)

Abstract

The results of two methods retrieving actinic flux and ozone photolysis frequencies from measurements of irradiance with a Brewer MKIII spectroradiometer are investigated in this paper. The first method uses actinic flux retrieved from irradiance measurements by the use of known formulas while the second is an empirical method converting irradiance to ozone photolysis frequencies through polynomials extracted from a study of synchronous actinic flux and irradiance measurements. When examining the actinic fluxes derived from the first method to those measured by an actinic flux spectrometer, data agree within ±10% for solar zenith angles lower than 75° for the UV-B and the UV-A wavelength band. Also, the actinic to global irradiance ratio derived, deviates within ±6% for solar zenith angles lower than 70° compared with cloudless sky calculations of the TUV model. For both cases the deviations are in the order of the magnitude of the measurements or model uncertainties. The ozone photolysis frequencies calculated by the second method show a mean ratio of 0.98±0.12 (1σ) and 0.97±0.06 for all data and for cloudless skies, respectively, when compared with ozone photolysis frequencies derived by a Bentham actinic flux spectroradiometer. Finally, the agreement of the two methods is within ±5% comparing two years' data of ozone photolysis frequencies retrieved from irradiance measurements at Thessaloniki, Greece. The use of such methods on extensive data sets of global irradiance can provide JO^1D values with acceptable uncertainty, a parameter of particular importance for chemical process studies.

1. Introduction

Solar ultraviolet radiation reaching the earth's surface is a fundamental parameter for atmospheric chemistry studies. It drives much of the tropospheric and stratospheric chemistry since the photodissociation frequencies of important chemical species are directly related to the incident radiation in this spectral region. In this way it contributes

ACPD

4, 4191–4225, 2004

to the removal of many trace gases as well as the generation of highly reactive radicals. For example, photodissociation of O_3 to O^1D in the presence of water vapor is a key reaction, controlling the oxidation capacity of the atmosphere through the formation of hydroxyl radicals (OH), while NO_2 photodissociation influences the removal rate of NO_x's and the ozone production in photochemical smog episodes.

Photolysis or photodissociation frequency of a species, J, represents the probability of photodissociation per second in a given radiation field. It is a function of the absorption cross section $\sigma(\lambda, T)$ (cm^2) of the parent molecule, the quantum yield $\phi(\lambda, T)$ of the photoproduct, which both depend on temperature, T and wavelength, λ, and the actinic flux F, (e.g. Madronich, 1987):

$$J = \int_{\lambda 1}^{\lambda 2} F(\lambda)\sigma(\lambda, T)\varphi(\lambda, T)d\lambda \quad (1)$$

The actinic flux, F, is the total number of photons incident at a point, (e.g. Madronich, 1987),

$$F(\lambda) \equiv \int_0^{2\pi} \int_0^{\pi/2} I(\lambda, \theta, \phi)\, \sin(\theta)\, d\theta\, d\phi = F_d(\lambda) + F_o(\lambda), \quad (2)$$

where $F_o(\lambda)$ and $F_d(\lambda)$ are the direct and diffuse radiance, respectively, incident on a spherical surface. The actinic flux describes the radiation incident on a spherical surface such as the molecules of the atmospheric species and is the suitable radiation quantity for photolysis frequencies determination.

Photolysis frequencies were measured in the past by means of chemical actinometry (Bahe et al., 1979; Dickerson et al., 1982; Junkermann et al., 1989; Blackbourne et al., 1992; Shetter et al., 1996) as well as filter radiometry (Dickerson et al., 1979; Bahe et al., 1979; Hofzumahaus et al., 1992; Shetter et al., 1996; Balis et al., 2002). Measurements of spectral actinic flux have started to develop since the 1990's (Müller et al.,

ACPD
4, 4191–4225, 2004

1995; Hofzumahaus et al., 1999; Shetter and Müller, 1999; Kraus and Hofzumahaus, 1998), and continued in various campaigns such as ADMIRA (Webb et al., 2002) and IPMMI (Bais et al., 2003). Spectroradiometric calculations of photolysis frequencies, using Eq. (1), were first reported by Müller et al. (1995) and Mc Elroy et al. (1995) and later by (Cotte et al., 1997; Shetter and Müller, 1999; McKenzie et al., 2002), establishing a more versatile method, since photolysis frequencies for different gases can be determined from the same actinic flux spectra providing that the cross section $\sigma(\lambda, T)$ and quantum yield $\phi(\lambda, T)$ functions are known. However, there are no long term series of photolysis frequencies derived from spectral actinic flux measurements, as most of the existing instruments have only been used for campaign purposes or short term experimental scientific projects.

Actinic flux measurements are not trivial. They require spectroradiometers with especially configured optics to enable measurements of radiation equally weighted from all directions. The most commonly measured quantity at UV monitoring sites, is the global irradiance, E, which is the radiation incident on a flat surface and can be expressed as:

$$E(\lambda) \equiv \int_0^{2\pi} \int_0^{\pi/2} I(\lambda, \theta, \phi) \cos(\theta) \sin(\theta) d\theta d\phi = E_d(\lambda) + E_o(\lambda), \quad (3)$$

where $I(\lambda, \theta, \phi)$ is the spectral radiance, θ and ϕ are the zenith and azimuth angles, respectively, $E_o(\lambda)$ is the direct irradiance and $E_d(\lambda)$ is the diffuse irradiance both incident on a horizontal surface. The irradiance describes the radiance on a horizontal surface integrated over the whole upper hemisphere, weighted with the cosine of the incidence angle.

UV monitoring networks have been developed worldwide for some years now, and have provided quality assured long-term series of spectral irradiance measurements. Regular spectral irradiance measurements have started in the late 1980's (Josefsson, 1986; Evans et al., 1987; Bais et al., 1993). Some examples of the longest records of

ACPD
4, 4191–4225, 2004

spectral UV measurements worldwide are those of Sodankylä, Finland (Masson and Kyrö, 2001), Thessaloniki, Greece (Zerefos et al., 2002), Hohenpeissenberg, Germany (Gantner et al., 2000) and Toronto, Canada starting in 1989 (Kerr and McElroy, 1993). In the absence of regular measurements of actinic flux, using irradiance data to determine photolysis frequencies with an acceptable uncertainty seems to be a promising method that would enable the production of long-term series of photolysis frequencies for the past, in UV measuring sites where only irradiance measurements are available.

The relationship between irradiance and actinic flux has been investigated (Madronich, 1987; Ruggaber et al., 1993; Van Weele et al., 1995) and empirical relationships have been derived for the retrieval of actinic flux from measurements of irradiance, aiming ultimately to photolysis frequency calculation. For the retrieval of actinic flux from irradiance, the ratio of the direct to global irradiance and the ratio of the diffuse actinic to diffuse global irradiance are required. Kazadzis et al., (2000), reported retrieved cloudless sky spectral actinic fluxes using measurements of global and direct irradiance which were in agreement with model calculations within ±5%, while Webb et al. (2002) introduced the use of modeled ratio of direct to global irradiance when no information of the direct irradiance is available. Kylling et al. (2003) tested an algorithm for converting irradiance to actinic flux against simultaneous measurements of actinic flux at four sites in Europe. The ratio of the reproduced to the measured actinic fluxes was 1.021±0.085 in the UVB and 1.015±0.105 in the UVA. Further studies have shown that photolysis frequencies determined by actinic fluxes and irradiances are in good agreement when the differences in the geometries are taken into account (McKenzie et al., 2002). Finally, there are studies estimating surface actinic flux from satellite ozone and cloud reflectivity measurements (Mayer et al., 1998).

In this paper, two methods for determining ozone photolysis frequencies $J(O^1D)$ from measurements of irradiance are presented and evaluated. The first method retrieves actinic flux from spectral measurements of irradiance. Retrieved actinic fluxes are compared with synchronous actinic flux measurements performed at Thessaloniki, Greece (40.64° N, 22.97° E, elevation 80 m) from July to December 2001. Ozone photolysis fre-

quencies from both actinic flux and irradiance measurements are then calculated and compared. The second method is a statistical way of calculating ozone photolysis frequencies from irradiance measurements using polynomials derived from synchronous measurements of actinic flux and global irradiance at Thessaloniki from April to July 2003.

This work is divided into four sections. The first describes the instruments, the locations where the measurements were performed and the data that were used. The second and third describe the two methods, discussing their results in comparison with other instruments. In the final section the two methods are compared and their differences are discussed.

2. Instrumentation and model data

The global and direct solar UV irradiance spectra used in this study, were measured with a double-monochromator Brewer MKIII spectroradiometer, which provides spectral UV irradiance measurements in the range of 287–366 nm. The calibration of the instrument is maintained by using, once a month, 1000-Watt working standards, whose absolute irradiance calibration is maintained by comparison, once every six months, to two 1000-Watt spectral irradiance standards traceable to the National Institute of Standards and Technology (NIST) standards. The uncertainty of the global irradiance measurements is within about ±5%, including the uncertainties of the calibration standards, the calibration transfer procedure and the overall instrument stability (Bais, 1997; Gardiner, 1997).

Spectral measurements of actinic flux (290–500 nm) were performed with a double-monochromator spectroradiometer developed by METCON Inc. (CVI Laser spectrograph with photomultiplier tube detector and actinic flux input optics with a Full Width at Half Maximum of 1 nm), which was installed on the roof of the Physics Department of the Aristotle University of Thessaloniki during the monitoring campaign of the ADMIRA (Actinic flux Determination from Measurements of Irradiance) project. It provided

ACPD
4, 4191–4225, 2004

simultaneous measurements with those of global irradiance measured by the Brewer spectroradiometer from January to December 2001. The uncertainty of the actinic flux measurements is estimated to about ±10%.

During the INSPECTRO (Influence of clouds on the Spectral actinic flux in the lower Troposphere) project, a Bentham DTM 300 (University of Innsbruck, Institute of Medical Physics) was installed at the same location and performed synchronous measurements of actinic flux and global irradiance from March to July 2003. The instrument has a slit function of 1 nm full width at half maximum (FWHM) and it is equipped with a Y-shaped fibre that is divided for actinic flux (from the upper hemisphere) and global irradiance input optics. Both input optics are rigged with a shutter that opens and closes the entrance of the fiber. With this set up both radiation quantities can be measured within seconds. Measurements are routinely performed from sunrise to sunset every half hour and wavelengths are scanned from 290–550 nm with a step size of 0.5 nm.

Model calculations were made with the Tropospheric Ultraviolet and Visible radiative transfer model (TUV) version 4.0, available by anonymous ftp from Sasha Madronich (1993), National Center for Atmospheric Research. In order to solve the radiation transfer equation, the DISORT method with 16 streams (Stamnes et al., 1988) was used. Actinic flux calculations were made with high wavelength resolution (0.05 nm) from 290 to 400 nm. All spectra were then convoluted with the slit function of the Brewer spectroradiometer. Total ozone and aerosol optical depth (AOD) measurements (at 340 nm) were used as model input data. Aerosol vertical profile from Shettle and Fenn (1979) and US standard profiles for air density, ozone and temperature (US, 1991) were used to simulate atmospheric composition and structure for all calculations. The single scattering albedo and asymmetry factor of aerosols were assumed, respectively, 0.85 and 0.70, independent of wavelength and height, while the Angstrom α coefficient was set to 2. Surface albedo was set to 0.03 and ATLAS 3 spectrum (Van Hoosier, 1996) was chosen as the extraterrestrial solar flux. Rayleigh cross-sections according to the analytical function of Nicolet (1984) and ozone cross-sections proposed by Bass and Paur (1985) were used in the model calculations.

ACPD
4, 4191–4225, 2004

A summary of the information on the instruments, the locations and the periods of the measurements that are used in both methods presented on this paper are shown in Table 1.

3. Actinic flux retrieval from measurements of irradiance

3.1. Description of the method

The methodology and the algorithms that were used for retrieving actinic flux spectra from irradiance measurements are described in Kazadzis et al. (2000). A brief description and the basic formulas used are summarized below.

If the spectral irradiance, $E(\lambda)$, is measured with a spectroradiometer, the downwelling actinic flux, $F(\lambda)$, can be derived from the following formula:

$$\frac{F}{E}(\lambda) = \left[A(\lambda) + f_{DG} \bullet \left(\frac{1}{\cos(x)} - A(\lambda)\right)\right], \quad (4)$$

where f_{DG} is the spectral ratio of direct to global irradiance, $A(\lambda)$ is the ratio of diffuse actinic flux to diffuse global irradiance and x is the solar zenith angle (sza).

f_{DG} can be determined spectrally by fitting a polynomial on measurements of this ratio at individual wavelengths. Such measurements, at 10 nm intervals, can be obtained from the Brewer spectroradiometer, by modifying its standard measurement protocol. During the measurement of a global irradiance spectrum, the Brewer performs a measurement of the direct solar irradiance every 10 nm (Bais et al., 1998). Since the solar zenith angle can be calculated from the time of the measurement, the only unknown parameter in Eq. (4) is $A(\lambda)$.

For cloudless sky conditions $A(\lambda)$ can be calculated with the aid of a radiative transfer model. Model calculations were used to investigate the sensitivity of A(λ) to wavelength (between 300 nm and 365 nm), to total ozone (300–400 D.U.), to aerosol optical depth at 340 nm (0.0–1.0) and to solar zenith angle (20°–80°). The parameter $A(\lambda)$ varies from

ACPD
4, 4191–4225, 2004

1.55 for low solar zenith angles and high AOD in the UVB, to 2.15 for very low AOD in the UVA. The dependence of A to total ozone column is very small. $A(\lambda)$ reaches a maximum at 55°–60° solar zenith angle for all wavelengths and aerosol optical depths. For the whole range of the AOD variation, $A(\lambda)$ on the average equals with 1.65±0.1 in the UV-B 1.90±0.25 in the UV-A.

For cloudy conditions $A(\lambda)$ slightly varies with wavelength and solar zenith angle, as it appeared from radiance measurements made in Thessaloniki under such conditions. A was derived from actinic fluxes and irradiances which were computed from the radiance measurements. These results for different wavelengths and solar zenith angles are summarized in Table 2.

Kylling et al. (2003) and Webb et al. (2002) assumed a constant value of 1.73 for the parameter $A(\lambda)$. When the diffuse sky radiance distribution is assumed isotropic, $A(\lambda)$ equals 2. The use of this assumption on Eq. (4) may introduce errors in the calculated actinic flux that can be as much as 17% for large solar zenith angles in the UVB.

3.2. Application of the method to measurements at Thessaloniki

The method described above was applied to 5 years of spectral irradiance measurements (1997–2002) made with a Brewer MKIII spectroradiometer in Thessaloniki, Greece. Over 18 000 global irradiance scans were converted to spectral actinic flux. The spectra measured under cloudy conditions were determined by combining hourly observations of the cloud cover from the local station of the National Meteorological Service and one-minute samples from a collocated pyranometer. The pyranometer data were used to determine the variability and the reduction of the radiation field during each scan (lasting for about 8 min) following a methodology proposed by Vasaras et al. (2000).

Ratios of retrieved actinic flux to global irradiance as a function of solar zenith angle are presented in Fig. 1, for two wavelengths 305 nm and 355 nm, representative of the UV-B and the UV-A, respectively.

This ratio is expected to be greater than unity, since irradiance refers to radiation

ACPD
4, 4191–4225, 2004

weighted with the cosine of the incidence angle, while actinic flux is equally weighted from every direction. On the average, the ratio F/E is 1.70±0.30 at 305 nm and 1.85±0.45 at 355 nm. In the UV-B, a minimum at small solar zenith angles and a maximum at solar zenith angles close to 65° are observed, corresponding to cloudless sky conditions. In the UV-A the maximum of F/E is larger, as a result of the greater contribution of the ratio f_{DG} at longer wavelengths (see Eq. 4). The variability of the ratio F/E at 305 nm at a certain solar zenith angle reaches a minimum (±3%) between 50° and 60° sza, increasing to about ±10% for smaller and larger solar zenith angles. The larger variability corresponds to cloudless sky conditions, while for broken clouds and overcast conditions the variability is smaller.

The variability of the ratio F/E for cloudless sky conditions is shown in Fig. 2, which presents averages values with their standard deviations for groups of 10° sza at 4 wavelengths. The smooth curves correspond to model calculations for the shortest and longest wavelengths. In the model constant values for ozone (350 D.U.) and AOD at 340 nm (0.5) were used, which both correspond to the observed average values of the two parameters in Thessaloniki. The model results are in good agreement with the measurements, within 1σ.

In general, F/E increases monotonically with increasing solar zenith angle, following the decreasing contribution of the direct component in the irradiance measurements. This dependence becomes more profound with increasing wavelength, because the contribution of the direct component becomes stronger in comparison to the diffuse component, both in actinic flux and irradiance. The combination of the two mechanisms results in higher F/E at 355 nm than at 305 nm at large solar zenith angles, while this feature reverses at small solar angles. The decrease of the F/E ratio after 70° is due to the fact that for this solar zenith angle the contribution of the direct component to the actinic flux becomes more important that the one in the global irradiance. So, by the decreasing direct sunlight reaching the ground, the ratio F/E decreases also.

ACPD
4, 4191–4225, 2004

3.3. Comparison of retrieved actinic fluxes with measurements from the METCON spectroradiometer and model calculations

Retrieved actinic fluxes from irradiance spectra measured with the Brewer spectroradiometer are compared to actinic flux spectra from the collocated METCON spectroradiometer. Both spectral measurements were synchronized to start at 5° sza intervals.

The maximum time difference between the two instruments when measuring the same wavelength was 2 min. This time difference could affect significantly the ratios under partly cloudy conditions, especially when rapidly moving clouds obscure momentarily the sun. Averages of actinic flux ratios for each solar zenith angle are shown in Fig. 3, separately for three wavelengths and for the ozone photolysis frequency.

In general, the agreement between the retrieved actinic fluxes and photolysis frequencies with the measurements is better than ±10% for solar zenith angles smaller than 70°. This level of agreement is within the uncertainties of the measurements and the retrieved data. At large solar zenith angles, although the averaged ratios are still within ±10%, the dispersion of the ratios (reflected in their standard deviation) is significantly larger. This may be attributed to various factors, such as the increased uncertainty of both types of measurements due to very low signals at large sza and short wavelengths, the non ideal angular response of the METCON instrument, and the higher uncertainty of the retrieval method under these conditions. On the average the ratio for all sza is approximately 0.95, and its deviation from unit, is caused by differences in the absolute scales (different calibration sources) of the two instruments and the overall calibration uncertainties. Finally, the wavelength variability of the average ratios is within ±5% for solar zenith angles lower than 80°.

As an additional test for validating the retrieval method and investigating its limitations, we compared the ratio F/E at 340 nm as retrieved from the Brewer spectroradiometer and as calculated by the TUV model. In this comparison measurements recorded only under cloudless skies were used, because under cloudy conditions it is impossible to measure the total ozone and the aerosol optical depth, and also be-

cause the model cannot reproduce with the same accuracy the radiation field under the clouds (mainly due to insufficient input parameters to describe the clouds). The model was run for each individual measurement, using as input the closest to global irradiance measurement total ozone and aerosol optical depth, which were retrieved from the classic direct sun (DS) measurement of the Brewer. The data used in this comparison were recorded at Thessaloniki during years 2000 and 2001. The results are shown in Fig. 4.

The reproducibility of the F/E ratio using the described method is in agreement within ±6% with the model calculations for solar zenith angles smaller than 70°. For solar zenith angles larger than 70° the uncertainty of the measurements and the model input parameters (aerosol optical depth, ozone, single scattering albedo) result to larger deviations. All results from Figs. 3 and 4 can be summarized in Table 3.

3.4. Uncertainty of the method

Based on Eq. (4), the uncertainty of the global irradiance measurements performed by the Brewer spectroradiometer is transferred almost directly to the retrieved actinic fluxes with very small wavelength dependence. The contribution of the uncertainty of the direct sun measurements is about ±7%, mostly for solar zenith angles between 40° and 65° and with a small (~2%) wavelength dependency.

If the angular distribution of the diffuse radiation field can not be characterized and $A(\lambda)$ cannot be derived from model calculations (due to the absence of in situ data that will used for the model input parameters), the diffuse radiation is assumed isotropic resulting to an overestimation of the retrieved spectral actinic fluxes (Kylling et al., 2003). Because in such a case $A(\lambda)$=2 a wavelength dependency of up to 10% is also introduced as we move from shorter to longer wavelengths. For measurements at sites with aerosol optical depth similar to Thessaloniki's, the isotropy assumption might increase the uncertainty of the retrieved actinic fluxes up to ±15%, whereas these uncertainties are much smaller at sites with small aerosol optical depth. Therefore, the use of the isotropy assumption is recommended only when no other information is available.

ACPD
4, 4191–4225, 2004

To conclude, the overall uncertainty of the retrieved actinic fluxes for cloudless skies and sza smaller than 70° using global and direct measurements and model calculated $A(\lambda)$, is about ±10% for the UV-B and ±12% in the UVA including the measurement and the retrieval uncertainty. Under broken cloud conditions, difficulties in determining the $A(\lambda)$ and f_{DG} parameters would increase these uncertainties. However, if f_{DG} is actually measured (as with our Brewer every 10 nm) and since the variability of $A(\lambda)$ in the presence of clouds is small, especially in the UVB, this additional uncertainty would be relatively small.

For sza smaller than 40° the uncertainty that is introduced by an extreme erroneous value of $A(\lambda)$ is less than 10%. For sza between 40° and 70° the error is estimated to 5% for 305 nm and 15% for 355 nm. For larger sza the uncertainty is smaller due to the small contribution of the term $[f_{DG}\ (1/\cos\theta - A)]$ in Eq. (4).

For overcast conditions the small variability of F/E for all wavelengths ensures that a good parameterization of parameter $A(\lambda)$ would eliminate any sources of uncertainties other than the ones of the actual irradiance measurement.

4. Statistical method for J(O^1D) calculation

4.1. Description of the method

The second method presented, aims at the direct determination of J(O^1D), merely by the use of global irradiance, through empirical relationships derived statistically from a dataset of synchronous measurements of actinic flux and global irradiance. The final calculation of J(O^1D), is based on a minimum number of parameters, in this case, global irradiance and solar zenith angle.

The method is based on the fact that the variability of the actinic flux to global irradiance ratio (F/E) due to aerosols and clouds for the same sza is relatively small in the UVB. Model calculations show that the variability of F/E in the UVB is within ±13% for all conditions and does not exceed ±8% for AOD changes from 0.2 to 1.0.

ACPD
4, 4191–4225, 2004

$J(O^1D)$ was calculated from the spectral actinic flux data from the Bentham spectroradiometer derived from Eq. (1). Also, using global irradiance instead of actinic flux in Eq. (1), a series of pseudo ozone photolysis frequencies (Jps) was produced. From these data the ratio $J(O^1D)$/Jps as a function of global irradiance in various wavelengths in the UV was examined. The global irradiance wavelength chosen as an independent variable was 325 nm, as being less affected by the seasonal variability of total ozone column and within the wavelength range of single monochromators Brewer spectroradiometers, which may be potentially used for $J(O^1D)$ retrievals. The ratio of $J(O^1D)$/Jps versus global irradiance at 325 nm using measurements from the Bentham spectroradiometer is presented in Fig. 5.

Evidently, this ratio strongly depends on solar zenith angle. Low values of the ratio, corresponding to high global irradiances are found at small solar zenith angles and the ratio increases with decreasing irradiance as we move to higher zenith angles. Apart from large sza, weak global irradiances may also correspond to measurements at small sza where clouds are present. This variability is attributed to the differences of global irradiance and actinic flux diurnal patterns, as shown in Fig. 1. For a certain solar zenith angle the spread of the points is related to the aerosol optical depth variations. In addition, for a certain sza and for the same irradiance at 325 nm, differences in the ratio originate from differences in the radiance distribution in the upper hemisphere.

The scope of the statistical method is to derive a statistical relation between $J(O^1D)$ and global irradiance, which would be used to calculate the ozone photolysis frequency from irradiance measurements. The dataset was divided into groups of 5° sza and 3rd degree polynomials were calculated from least squares fits between the measured $J(O^1D)$ and global irradiance at 325 nm (E_{325}). Using these polynomials we recalculated for the whole period the ozone photolysis frequencies (Jcalc). The average ratio between measured and calculated J's ($\frac{Jcalc}{J(O^1D)}$) was found to 1.007±0.028, for all solar zenith angles and all sky conditions (Fig. 6).

To check the consistency of the method the polynomials were also calculated using the first half of the data set and applied to the almost independent second half. The

ACPD
4, 4191–4225, 2004

comparison of the recalculated ozone photolysis frequencies for the second period with the measured $J(O^1D)$ revealed that the mean value of the ratio $\frac{Jcalc}{J(O^1D)}$ was 1.002±0.031, giving confidence that the derived polynomials may be used satisfactorily to reproduce the measurements.

The variability of the ratio in Fig. 6 is related to the uncertainty introduced by the use of the polynomials. Also, when rapid changes of the radiation field occur due to fast moving clouds in front of the sun, the atmospheric conditions at the time of the 325 nm irradiance measurement could differ from those at the time of the spectral actinic measurement used for the ozone photolysis calculation.

4.2. Comparisons of $J(O^1D)$ retrieved from different instruments

The next step was to apply the $J(O_1D)$ retrieval method to the global irradiance data from the Brewer MKIII spectroradiometer, which operates regularly at the Laboratory of Atmospheric Physics in Thessaloniki. A laboratory investigation of the calibration standards used by the two instruments (Brewer and Bentham) showed a difference of ∼8% at 300 nm and ∼3% at 360 nm. Therefore the Brewer measurements were adjusted spectrally by the ratio of the lamp measurements to make the measurements of the two instruments comparable. Due to the differences in the instrument's slit functions all data were corrected for possible wavelength shifts using the SHICRIVM (Slaper et al., 1995) algorithm and a deconvolution of the measured spectra to a standard slit with 1 nm FWHM was calculated.

Jbrw denotes the photolysis frequencies calculated from the Brewer global irradiance spectral measurements by applying the above described retrieval method. The corresponding ratio $\frac{Jbrw}{J(O^1D)}$ is shown in Fig. 7.

The ratio is slightly below unity. Similar differences were also observed in the comparison of global spectral irradiance data from the two instruments, which in the UVB was 0.97±0.04. The reason for this small difference is attributed to the different location of the global irradiance heads of the two instruments, with the Bentham's head being

ACPD
4, 4191–4225, 2004

2.5 m higher from the Brewer's and with much clearer horizon. The surrounding buildings obscure a small fraction of the diffuse sky light to reach the instruments heads, but this fraction is slightly higher for the Brewer (~2% for isotropic radiation). The main reason for the dispersion of the ratios around unity could be the small time difference (the order of a few seconds) between the scans, something that can be more significant during partly cloudy conditions. The mean ratio is 0.98±0.12 (1σ) and 0.97±0.06 for all data and for cloudless skies, respectively.

The polynomials derived from the four-month monitoring INSPECTRO campaign in Thessaloniki were then applied to Bentham's global irradiance data recorded during the INSPECTRO campaign in Weybourne, UK, to investigate the validity of the method for other sites. The ratio of the photolysis frequency, Jcalc, as calculated from the polynomials, to $J(O^1D)$ derived from the spectral actinic flux measurements is shown as a function of solar zenith angle in Fig. 8, and it is on the average 0.99±0.05.

It appears that there is no systematic dependence of the ratio on solar zenith angle. The atmospheric pattern for this 17-day period was dominated by partly cloudy and overcast sky conditions, with occasional clear sky intervals. The application of the method to this data set showed generally good agreement among measured and calculated ozone photolysis frequencies, although the dispersion of the ratios around unity is almost double compared to the similar plot derived for Thessaloniki (Fig. 6).

It should be noted that the errors related to the accuracy of the $J(O^1D)$ determination for both Figs. 6 and 8 are linked only to the method uncertainties and not to any instrument problems during the periods of the measurements.

Under cloudless sky conditions and small solar zenith angles the calculated frequencies are underestimated by up to 8%. This could be a result of using the polynomials that were determined at urban area of Thessaloniki, where the atmospheric radiance characteristics are much different from those at Weybourne.

ACPD
4, 4191–4225, 2004

5. Comparison of the two methods

Photolysis frequencies of ozone (Jrtv) are calculated by weighting the retrieved actinic flux spectra from irradiance spectra (method 1) with the absorption cross-section of ozone (Bass and Paur, 1985) and quantum yield (Shetter et al., 1997), for the period February 2000–December 2001. These results were compared to the values of Jcalc that have been calculated statistically (method 2) and their ratio as a function of time is presented in Fig. 9.

In Fig. 9 only data recorded at solar zenith angles smaller than 85° are shown. The ratio is independent of solar zenith angle or atmospheric conditions, with a mean value of 1.013±0.038 (1σ). For cloudless sky conditions the mean ratio is 1.021±0.030. The variability of the ratio is within the individual uncertainties of the two methods described above.

In Fig. 10 local noon values of ozone photolysis frequencies calculated by the two methods are presented, together with their monthly averages. Their difference is within ±3% for the entire period. The observed variability of JO^1D is a combined effect of the annual variability of solar zenith angle at local noon, total ozone column and clouds. JO^1D reaches a maximum of about $3.2510^{-5}\,s^{-1}$ in late June and beginning of July at Thessaloniki, Greece.

6. Conclusions

A simple algorithm for converting spectral UV irradiance to actinic flux was proposed and applied to five years of measurements performed by a Brewer spectroradiometer at Thessaloniki, Greece. The derived actinic flux to global irradiance ratio shows a solar zenith angle dependence, which is more pronounced in the UV-A wavelength band and for cloud free conditions.

The retrieved actinic fluxes at 340 nm agree with model calculations to within ±6% for solar zenith angles smaller than 70°. For larger solar zenith angles the differences

ACPD
4, 4191–4225, 2004

are within ±18%. Part of this difference can be explained by the uncertainty in the model input parameters. The retrieved ozone photolysis frequencies agree with those calculated from the measured actinic fluxes with a METCON instrument to within ±10% for solar zenith angles smaller than 75°, increasing to ±25% for larger solar zenith angles. The uncertainty of the METCON actinic flux spectroradiometer is estimated to ±10%, including the absolute calibration and the stability of the instrument.

A second, empirical, method for calculating $J(O^1D)$ which is based on solar zenith angle and measurements of global irradiance at 325 nm is presented. The ratio of $J(O^1D)$ derived from this method to that calculated directly from actinic flux spectra is very close to 1 with a standard deviation of less than 3% for solar zenith angles up to 60°. No evident dependence of the method on aerosol optical depth or total ozone column was found, which makes is suitable for use under different atmospheric conditions.

The ozone photolysis frequencies retrieved from measurements of actinic flux from a Bentham spectroradiometer were compared to those calculated using retrieved actinic flux from irradiance measurements recorded by a collocated Brewer spectroradiometer. It was observed that the level of their agreement is similar to that of the global irradiance spectra measured by the two instruments. The standard deviation of their global irradiance ratios is ∼4%, while for the photolysis frequency it is ∼6% and ∼12%, respectively, for cloud free and all conditions. The results from the two methods agree to within ∼4%, which is within the limits of their uncertainties.

UV monitoring stations distributed worldwide provide long-term series of global irradiance measurements. The need for reliable ozone photolysis frequencies, as an important input parameter for global tropospheric chemical transport models, combined with the absence of regular actinic flux measurements, calls for the development of methods for $J(O^1D)$ retrieval from measurements of irradiance. The accuracy of the retrieved data using the two methods presented in this paper is comparable to that of chemical actinometers measuring JO^1D (Shetter et al., 1996; Müller et al., 1995). The use of such methods on extensive data sets of global irradiance can provide JO^1D

ACPD
4, 4191–4225, 2004

values with acceptable uncertainty, a parameter of particular importance for chemical process studies.

Acknowledgements. Part of the work was conducted in the framework of the ADMIRA EVK2-1999-00018 project and the INSPECTRO EVK2-2001-00135 project, funded by the European Commission.

References

Bahe, F. C., Marx, W. N., Schurath, U., and Roth, E.: Determination of the absolute photolysis rate of ozone by sunlight, $O_3+h\nu \rightarrow O(^1D) + O_2(^1\Delta_g)$, at ground level, Atmos. Environ., 13, 1515–1522, 1979.

Bais, A. F.: Spectrometers: Operational errors and uncertainties, in Solar Ultraviolet Radiation, Modelling, Measurements and Effects, edited by Zerefos, C. S. and Bais, A. F., NATO-ASI Series, vol. 52, 165–174, 1997.

Bais, A. F., Zarefos, C. S., Meleti, C., Ziomas, I. C., and Tourpali, K.: Spectral measurements of solar UVB radiation and its relations to total ozone, SO_2 and clouds, J. Geophys. Res., 98, 5199–5204, 1993.

Bais, A. F., Kazadzis, S., Balis, D. S., Zerefos, C. S., and Blumthaler, M.: Correcting global solar UV spectra recorded by a Brewer spectroradiometer for its angular response error, Appl. Opt., 37, 6339–6344, 1998.

Balis, D. S, Zerefos, C. S, Kourtidis, K., Bais, A. F, Hofzumahaus, A., Kraus, A., Schmitt, R., Blumthaler, M., and Gobbi, G. P.: Measurements and modeling of photolysis rates during the Photochemical Activity and Ultraviolet Radiation (PAUR) II campaign, J. Geophys. Res., 107 (D0), doi:10.1029/2000JD000136, 2002.

Bass, A. M. and Paur, R. J.: The ultraviolet cross-section of ozone: I. The measurements, in Atmospheric Ozone, Proc. Quadrennial Ozone Symposium, edited by Zerefos, C.S. and Ghazi, A., Reidel publ., 601–606, 1985.

Blackburn, T. E., Bairai, S. T., and Stedman, D. H.: Solar photolysis of ozone to singlet D oxygen atoms, J. Geophys. Res., 97, 10 109–10 117, 1992.

Cotté, H., Devaux, C., and Carlier, P.: Transformation of irradiance measurements into spectral actinic flux for photolysis rates determination, J. Atmos. Chem., 26, 1–28, 1997.

Dickerson, R. R., Stedman, D. H., Chameides, W. L., Crutzen, P. J., and Fishman, J.: Actinometric measurements and theoretical calculations of $J(O_3)$, the rate of photolysis of ozone to $O(^1D)$, Geophys. Res. Lett., 11, 833–836, 1979.

Dickerson, R. R., Stedman, D. H., and Delany, A. C.: Direct measurements of ozone and nitrogen dioxide photolysis rates in the troposphere, J. Geophys. Res., 87, 4933–4946, 1982.

Evans, W. F. J., Fats, H., Forrester, A. J., Henderson, G. S., Kerr, J. B., Vupputuri, R. K. R., and Wardle, D. I.: Stratospheric ozone science in Canada: An agenda for research and monitoring, Environ Can., Rep ARD 87-3, Atmos. Environ. Serv., Dowsview, Ontario, Canada, 127, 1987.

Gardiner, B. G.: Spectroradiometer calibration methods and techniques, in Solar Ultraviolet Radiation, Modelling, Measurements and Effects, edited by Zerefos, C. S. and Bais, A. F., NATO-ASI Series, vol. 52, 165–174, 1997.

Hofzumahaus, A., Brauers, T., Platt, U., and Callies, J.: Latitudinal variation of measured O^3 photolysis frequencies $J(O^1D)$ and primary OH production rates over the atlantic ocean between 50° N and 30° S, J. Atmos. Chem. 15, 283–298, 1992.

Hofzumahaus, A., Kraus, A., and Mueller, M.: Solar actinic flux spectroradiometry: A technique for measuring photolysis frequencies in the atmosphere, Appl. Opt., 38, 4443–4460, 1999.

Josefsson, W.: Solar ultraviolet radiation in Sweden, SMHI Rep. Meteorol. Climatol., No. 53, Swed. Meteorol. And Hydrol. Indt., Norrkoping, Sweden, 72, 1986.

Junkermann, W., Platt, U., and Volz-Thomas, A.: A photoelectric detector for the measurement of photolysis frequencies of ozone and other atmospheric molecules, J. Atmos. Chem., 8, 203–227, 1989.

Kazadzis, S., Bais, A. F., Balis, D., Zerefos, C. S., and Blumthaler, M.: Retrieval of downwelling UV actinic flux density spectra from spectral measurements of global and direct solar UV irradiance, J. Geophys. Res., 105, 4857–4864, 2000.

Kerr, J. B. and McElroy, C. T.: Evidence for large upward trends of ultraviolet-B radiation linked to ozone depletion, Science, 262, 1032–1034, 1993.

Kraus, A. and Hofzumahaus, A.: Field measurements of atmospheric photolysis frequencies for O_3, NO_2, HCHO, CH_3CHO, H_2O_2 and HONO by UV spectroradiometry, J. Atmos. Chem., 31, 161–180, 1998.

Kylling, A., Webb, A. R., Bais, A. F., Blumthaler, M., Schmitt, R., Thiel, S., Kazantzidis, A., Kift, R., Misslebeck, M., Schallhart, B., Schreder, J., Topaloglou, C., Kazadzis, S., and Rimmer, J.: Actinic flux determination from measurements of irradiance, J. Geophys. Res., 108(D16),

ACPD

4, 4191–4225, 2004

4506, doi:10.1029/2002JD003236, 2003.
Madronich, S.: Photodissociation in the Atmosphere: 1. Actinic Flux and the Effects of Ground Reflections and Clouds, J. Geophys. Res., 92, D8, 9740–9752, 1987.
Madronich, S.: The atmosphere and UV-B radiation at ground level, In: Environmental UV Photobiology, Plenum Press, New York, 1–39, 1993.
McElroy C. T., Midwinter, C., Barton, D. V., and Hall, R. B.: A comparison of J-values from the composition and photodissociative flux measurements with model calculations, Geophys. Res. Lett., 22, (11), 1365–1368, 1995.
McKenzie, R. L., Johnston, P. V., Hofzumahaus, A., Kraus, A., Madronich, S., Cantrell, C., Calvert, J., and Shetter, R.: Relationship between photolysis frequencies derived from spectroscopic measurements of actinic fluxes and irradiances during the IPMMI campaign, J. Geophys. Res., 107 (D5), 4042, doi:10.1029/2001JD000601, 2002.
Müller, M., Kraus, A., and Hofzumahaus, A.: $O_3 \rightarrow O(_1D)$ photolysis frequencies determined from spectroradiometric measurements of solar actinic UV-radiation: Comparison with chemical actinometer measurements, Geophys. Res. Lett., 22, 6, 679–682, 1995.
Nicolet, M.:On the molecular scattering in the terrestrial atmosphere: an empirical formula for its calculation in the homosphere, Planet. Space Sci., 32, 1467–1468, 1984.
Ruggaber, A., Forkel, R., and Dlugi, R.: Spectral actinic flux and its ratio to spectral irradiance by radiation transfer calculations, J. Geophys. Res., 98, 1151–1162, 1993.
Shetter, R. E. and Müller, M.: Photolysis frequency measurements using actinic flux spectroradiometry during the PEM-Tropics mission: Instrument description and some results, J. Geophys. Res., 104, 5647–5661, 1999.
Shetter, R. E, Cantrell, C. a., Lantz, K. O., Flocke, S. J., Orlando, J. J., Tyndall, G. S., Gilpin, T. M., Fischer, C. A., Madronich, S., and Calvert, G.: Actinometric and radiometric measurement and modelling of the photolysis rate coefficient of ozone to $O(^1D)$ during Mauna Loa Observatory Photochemistry Experiment 2, J. Geophys. Res., 101, 9, 14 631–14 641, 1996.
Shettle, P. and Fenn, R. W.: Models for the aerosols of the lower atmosphere and the effects of humidity variations on these optical properties, AFGL-TR-79-0214, Air Force Geophysics Laboratory, Hanscom AFB, Mass, 1979.
Slaper, H., Reinen, H. A. J. M., Blumthaler, M., Huber, M., and Kuik, F.: Comparing ground-level spectrally resolved solar UV measurements using various instruments: a technique resolving effects of wavelength shift and slit width, Geophys. Res. Lett., 22, 2721–2724, 1995.
Stamnes, K., Tsay, S.-T., Wiscombe, W., and Jayaweera, K.: Numerically stable algorithm for

ACPD
4, 4191–4225, 2004

discrete-ordinate-method radiative transfer in multiple scattering and emitting layered media, Appl. Opt., 27, 2502–2509, 1988.
United Nations Environment Program (UNEP): Environmental Effects on Ozone Depletion: 1991 Update, 1991.
US Standard Atmosphere 1976: US Government printing Office, Washington D.C., 1976.
Van Hoosier, M. E.: The Atlas-3 solar spectrum, available via anonymous ftp (ftp://susim.nrl.navy.mil), 1996.
Van Weele, M., de Arleeano, J. V.-G., and Kuik, F.: Combined measurements of UV-A actinic flux, UV-A irradiance and global radiation in relation to photodissociation rates, Tellus, Ser. B, 47, 333–364, 1995.
Webb, A. R., Kift, R., Thiel, S., and Blumthaler, M.: An empirical method for the conversion of spectral UV irradiance measurements to actinic flux data, Atmos. Environ., 36, 4044–4397, 2002.
Zerefos, C. S.: Long-term ozone and UV variations at Thessaloniki, Greece, Physics and Chemistry of the earth, 27, 455–460, 2002.

ACPD
4, 4191–4225, 2004

Table 1. Description of instruments details, location and periods of measurements.

Instrument	Measurement Quantity	Location	Period
METCON CVI Laser spectrograph	Actinic flux 290–500 nm	Thessaloniki, Greece	January–December 2001
Brewer spectroradiometer	Global irradiance 287–366 nm	Thessaloniki, Greece	1997–2003
Bentham DTM300	Actinic flux 290–550 nm Global irradiance 290–550 nm	Thessaloniki, Greece	March–July 2003
		Weybourne, UK	September 2002

ACPD
4, 4191–4225, 2004

Table 2. Mean values of A(λ) for different wavelengths and solar zenith angles under cloudy conditions.

wavelength (nm)	sza = 20°	sza = 40°	sza = 60°
305	1.65	1.68	1.70
320	1.70	1.72	1.75
340	1.70	1.72	1.75
355	1.70	1.72	1.75

ACPD
4, 4191–4225, 2004

Table 3. Comparison of retrieved F/E ratios and actinic fluxes with measurements (all atmospheric conditions) and model calculations (cloudless sky cases) as a function of solar zenith angle.

Solar zenith angle (±5°)	Ratios (F/E) at 340 nm Brewer/Model	Standard deviation	Metcon/Brewer (JO^1D)	Standard deviation
30	0.979	0.058	0.948	0.072
40	0.979	0.062	0.978	0.050
50	0.988	0.037	0.956	0.070
60	0.991	0.036	0.942	0.101
70	1.058	0.079	0.898	0.166
80	1.120	0.184	1.033	0.290

ACPD
4, 4191–4225, 2004

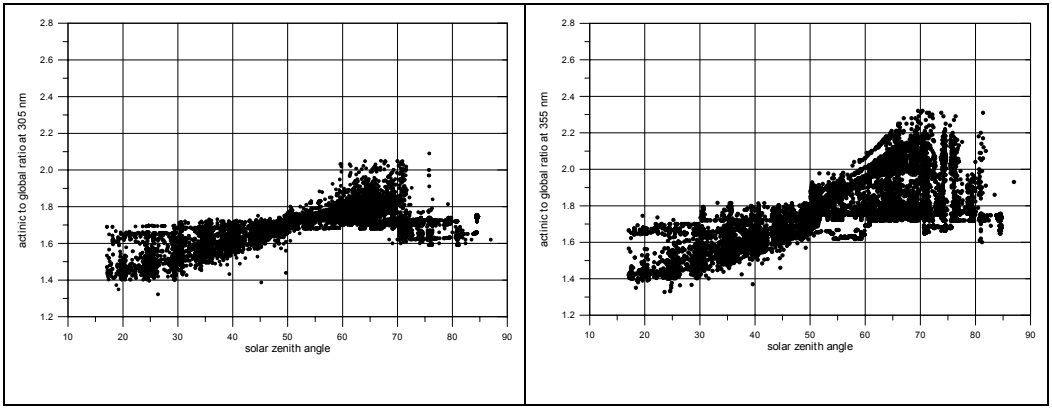

Fig. 1. Ratio of retrieved actinic flux to global irradiance at 305 nm (left) and 355 nm (right) retrieved from 1997–2002 at Thessaloniki, Greece.

ACPD
4, 4191–4225, 2004

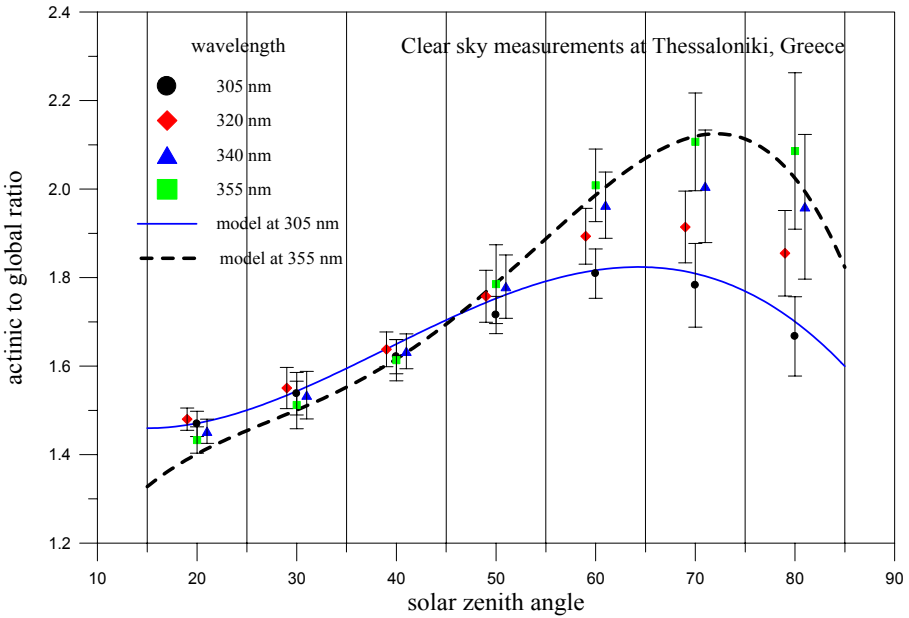

Fig. 2. Actinic to global ratio means for solar zenith angle groups of 10° at 305 nm (circles), 320 nm (diamonds), 340 nm (triangles) and 355 nm (boxes). Model calculations at 305 nm (solid line) and 355 nm (dash line). All data represent cloudless sky measurements.

ACPD
4, 4191–4225, 2004

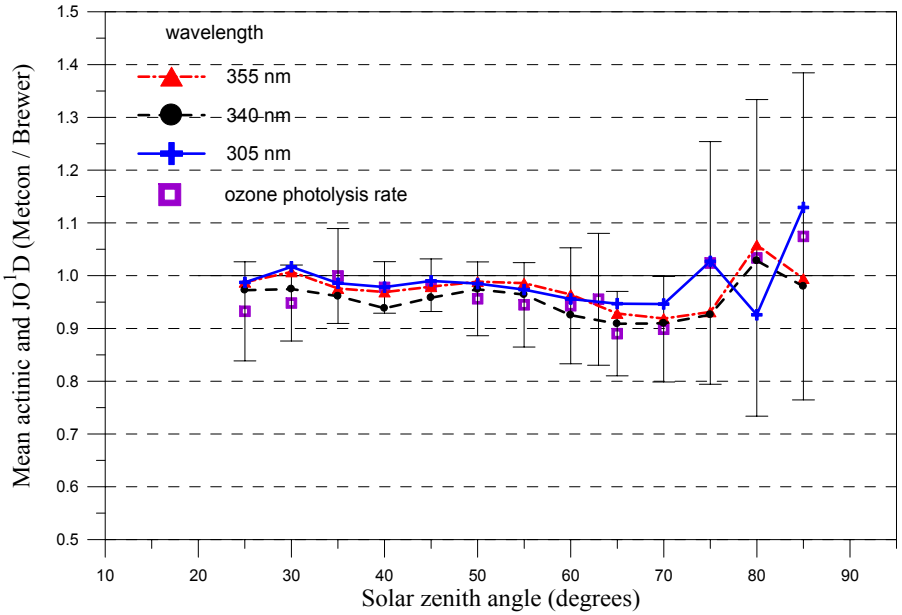

Fig. 3. Mean ratios of actinic fluxes measured by METCON and retrieved from the Brewer irradiances at 305±2 nm (crosses), 340±2 nm (circles), 355±2 nm (triangles) and of ozone photolysis frequencies (boxes), as a function of solar zenith angle (5° increments). The standard deviation for each solar zenith angle is shown only for 305 nm, representing the highest possible variability of the ratios.

ACPD
4, 4191–4225, 2004

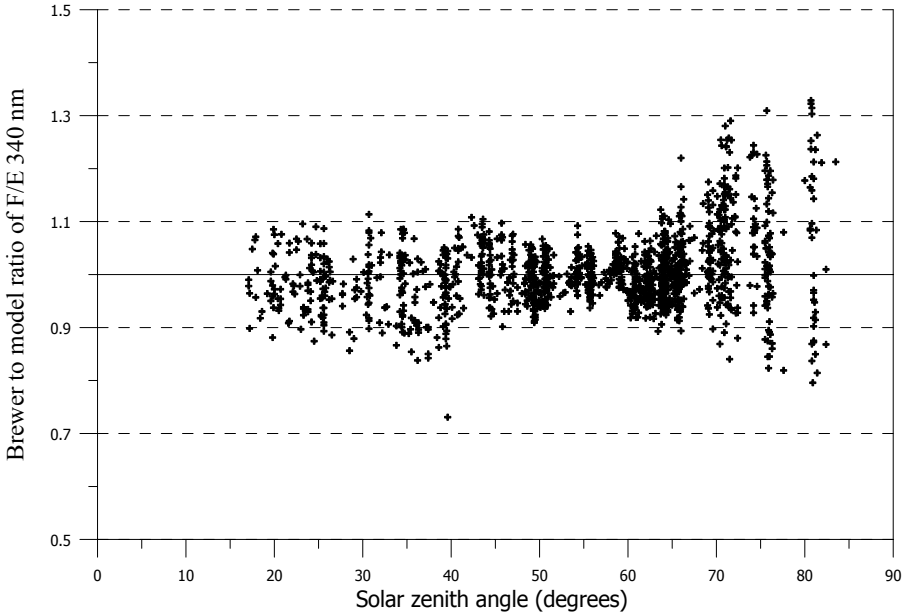

Fig. 4. Ratios of actinic to global irradiance at 340±2 nm as measured/retrieved from the Brewer and calculated with the TUV model. Measurements represent cloudless sky cases.

ACPD
4, 4191–4225, 2004

Actinic flux and O^1D photolysis frequencies at Thessaloniki, Greece

S. Kazadzis et al.

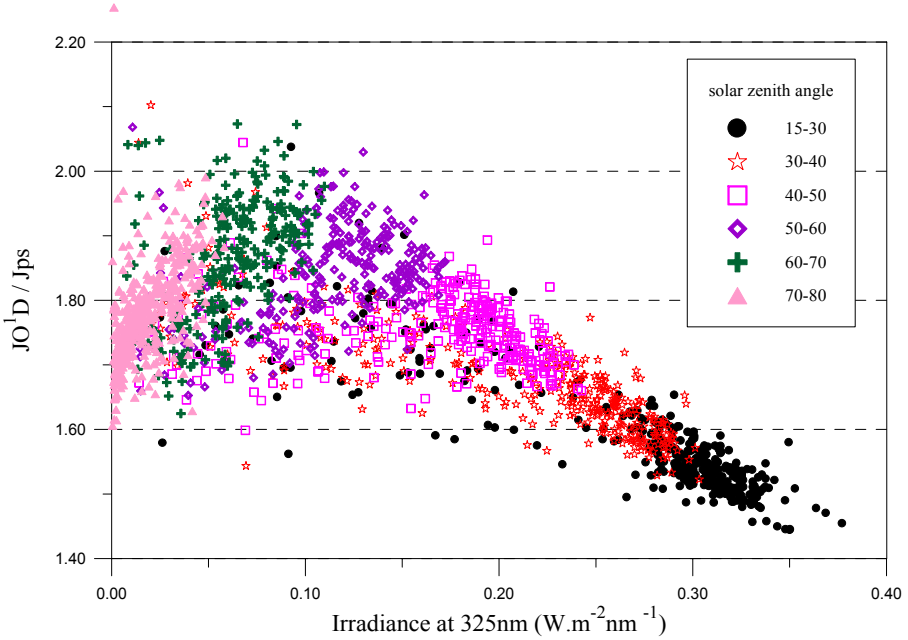

Fig. 5. Ratio of J(O^1D)/Jps, as a function of global irradiance at 325 nm for different groups of solar zenith angles. (J(O^1D) was calculated from the spectral actinic flux data from the Bentham spectroradiometer and Jps is calculated if the global irradiance is used instead of actinic flux in the formula given in Eq. 1.)

ACPD
4, 4191–4225, 2004

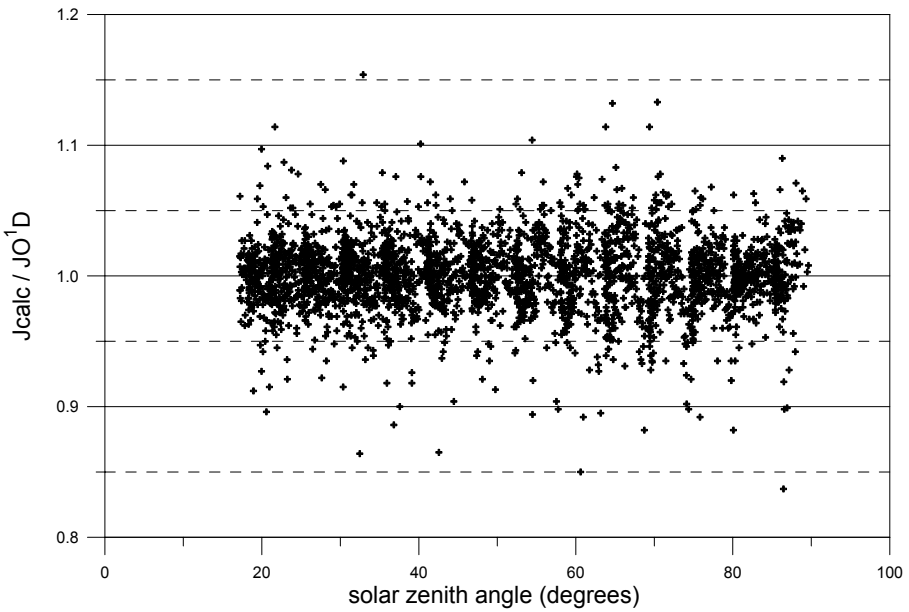

Fig. 6. Ratio of $\frac{\text{Jcalc}}{\text{J(O}^1\text{D)}}$ as a function of solar zenith angle from the Bentham's measurements data set. (Jcalc is calculated with method 2 using the global irradiance data and J(O^1D) using actinic flux spectra.)

ACPD
4, 4191–4225, 2004

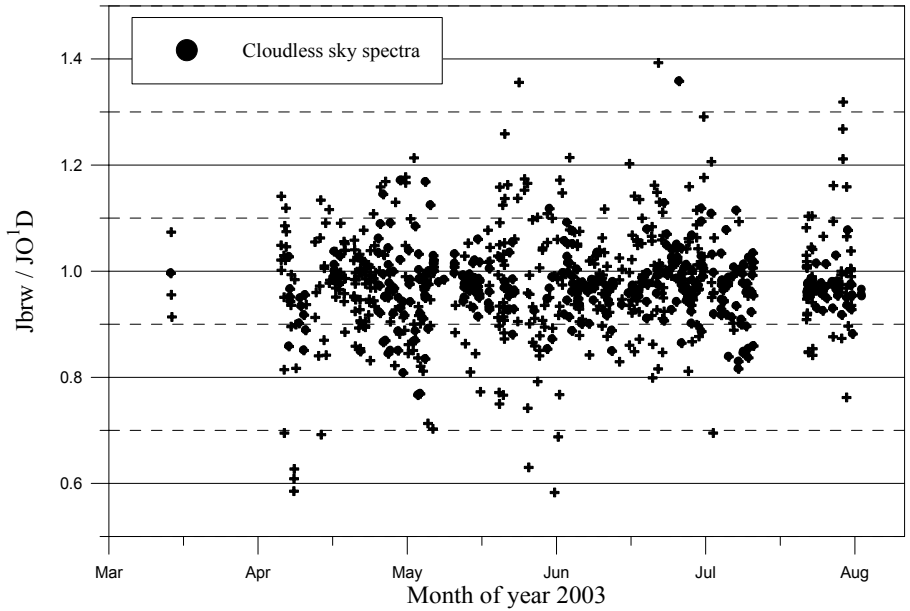

Fig. 7. $\frac{Jbrw}{J(O^1D)}$ ratio using global irradiance from Brewer MKIII. Circles represent measurements under cloudless sky conditions and crosses represent all measurements. (Jcalc is calculated with method 2 using the global irradiance data and $J(O^1D)$ using actinic flux spectra from the Bentham instrument.)

ACPD
4, 4191–4225, 2004

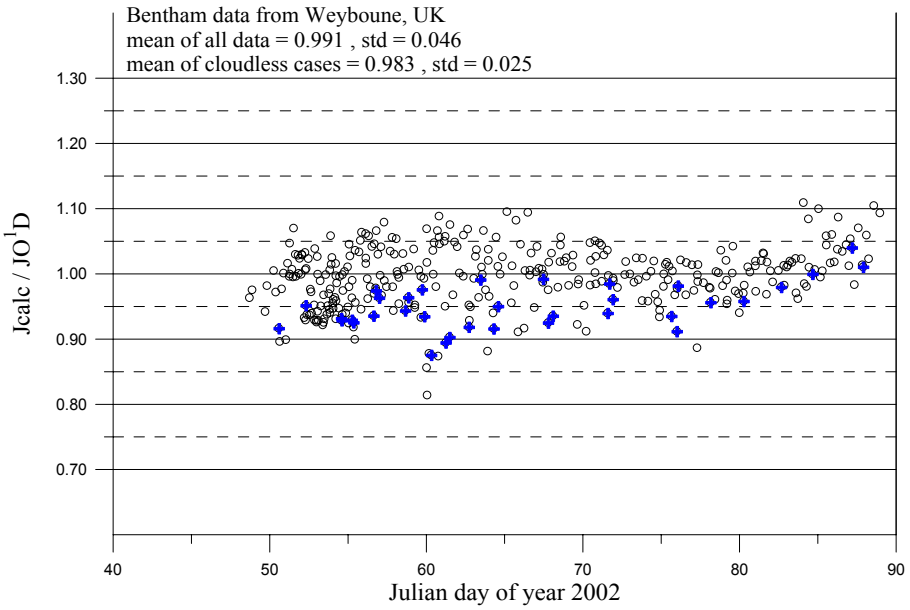

Fig. 8. Ratio of calculated J to J(O^1D) derived from global irradiance and actinic flux measurements from BENTHAM measurements at Weybourne, UK, as a function of solar zenith angle. Asterisks denote measurements under cloudless conditions.

ACPD
4, 4191–4225, 2004

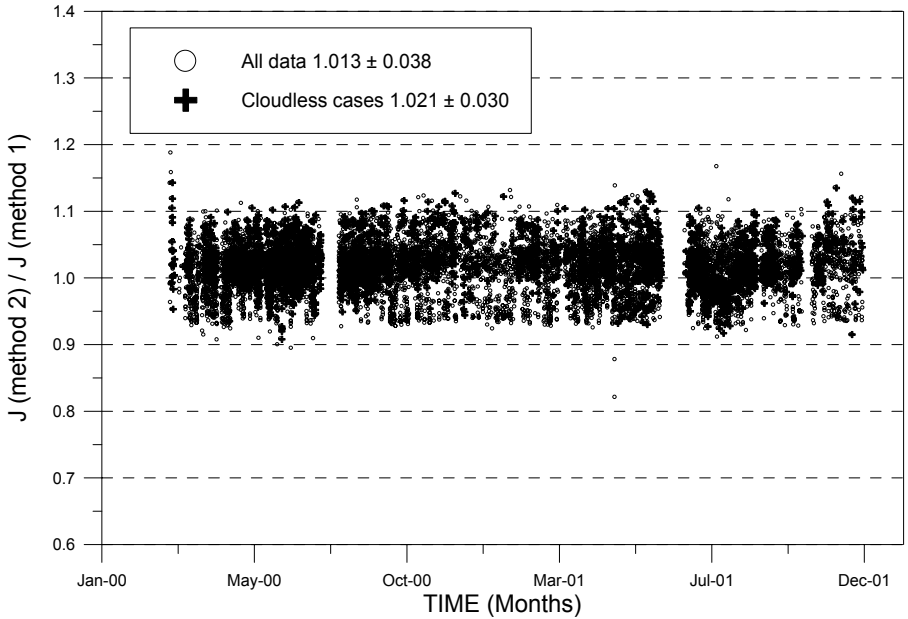

Fig. 9. Comparison of the ozone photolysis frequencies retrieved from the two methods described. Jcalc/Jrtv ratio during the period February 2000–December 2001 calculated for Thessaloniki. Circles represent the full data set and crosses the cloudless sky cases.

ACPD
4, 4191–4225, 2004

Actinic flux and O^1D photolysis frequencies at Thessaloniki, Greece

S. Kazadzis et al.

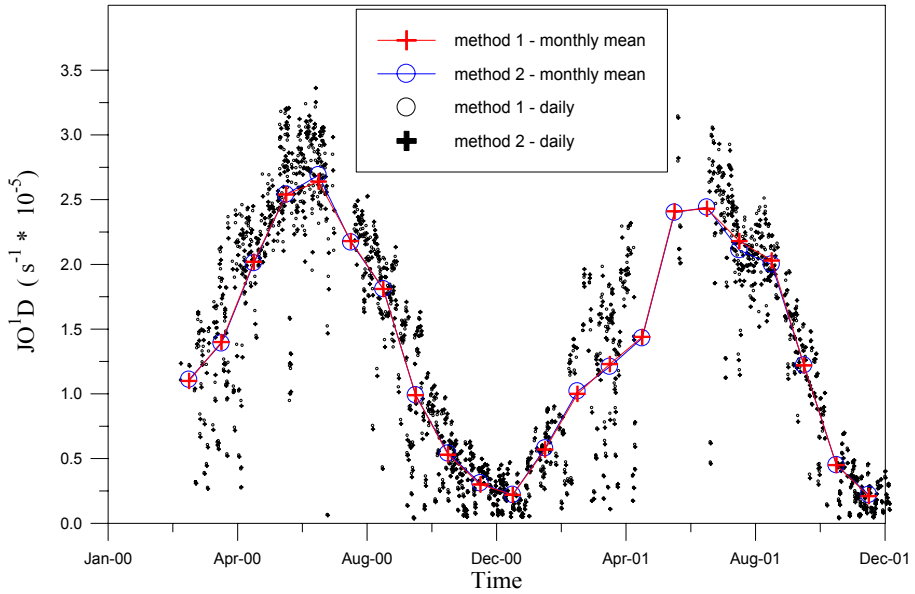

Fig. 10. Calculated JO^1D during local noon for the period February 2000–December 2001, at Thessaloniki following the two retrieval methods. Monthly averages are also shown.

ACPD
4, 4191–4225, 2004